FoMR
Frontiers of Multidisciplinary Research

Vol. 1 | No. 3 | Jul - Sep 2026

Analyzing Loss Mechanism of High Frequency Ferrite Core Transformer in Power Electronics Based Converter

Vivek Shrivastava[a], Sameer Bhambri[b]*, Manoj Kumawat[c]

ABSTRACT

The paper proposes an approach to design a high frequency ferrite core K-winding transformer in power electronics based applications with an objective to reduce both copper and core loss. The core loss in a high frequency transformer is controlled by operating flux density rather than saturation. Therefore, in substantial class of applications, it is necessary to model and limit core loss component through reducing peak ac flux density. The practical challenges in power electronics are addressed, particularly in efficiency and transformer design is improved by introducing optimization. In this paper, the core geometrical constant (K_g) of a magnetic device is generalized, leading to the geometrical constant (K_{gfe}), a measure of the effective magnetic size of a core in transformer design. A step-by-step guide for replicating the methodology is provided. The Design of a transformer core has been turned into an optimization problem, which is solved for variables such as mean length per turn, window area, core cross section area, window space fraction and mean length of magnetic path, that results in minimum total loss with inequality and equality constraints. A metaheuristics based algorithm, particle swarm optimization, in this case is applied to solve objective function which results in significant reduction in total loss occurred in core and winding. Different dimensions of EE type ferrite core are then estimated based on these optimized variables.

Received date: 28.11.2025
Accepted date: 30.05.2026

Keywords: Copper loss, Core loss, Design, Magnetic, Transformer

https://doi.org/10.65601/FoMR.2026.1.3.5

[a]*Electrical Engineering,*
National Institute of Technology, Uttrakhand

***Corresponding Author:**
[b,c]*Electrical Engineering,*
National Institute of Technology, Delhi
Email: sameerbhambri@nitdelhi.ac.in

1. INTRODUCTION

The excellent efficiency based properties of ferrite-based magnetics make them widely used in high-frequency DC-DC converters. Power converter designs based on HF (high frequency) transformers have seen a significant increase in attention due to the recent spike in interest in EVs (Electric vehicles), renewable energy integration, and associated infrastructure. The so-called K_g (core geometrical constant) approach and the AP (area-product) method are two popular transformer design techniques available in the literature. The design of magnetics is an essential and integral part that must be given importance in the production process of any switching converter and cannot be looked isolated. It is equally important for a power electronics engineer to model and design the magnetics apart from other designing aspects of converter (Erickson & Maksimovic, 2020). The K_g technique is employed in designing thermally conscious high frequency inductors. A Filter inductor design procedure through K_g method is elaborated with basic magnetics theory. The design is accomplished with prior knowledge of specified flux density and attained copper loss. Calculation of airgap, number of turns and conductor size are computed after selecting K_g which is an effective electrical size of core. The same method has been extended to the design of multi winding coupled inductor with an objective of minimizing overall winding copper loss. The result of the design reveals that total copper loss is minimized under the condition when window area is allocated between the windings according to their apparent powers (Bhambri et al., 2022; Dhole et al., 2021). whereas AP (area product) method that concentrates on the device's electromagnetic behavior, is also utilized (Atalla et al., 2016; Bhambri et al., 2022; Dhole et al., 2021; Iyer et al., 2015; Kudaravalli et al., 2022; Parikshith et al., 2010; Venkatramanan et al., 2013).

The thermal behavior of high frequency ferrite core transformer is investigated through providing theoretical perspectives and then experimental results from a hardware setup, but in the vast class of applications, core losses are significant as these are limited by peak flux density rather than saturation. Therefore, core losses are required to be modeled along with copper losses. The detailed design procedure of a multi winding inductor for multiple output full bridge buck converter has been explained in which designing procedure starts with selecting K_{gfe}, a geometrical constant satisfying an inequality. Then total losses are calculated followed by determination of peak ac flux density. Window space fractions are also determined for each winding (Roja et al., 2024; Erickson & Maksimovic, 2020).

The review of various magnetic circuits, inductor modeling, and transformer modeling has been provided in (Dauhajre & Middlebrook, 1986; MIT Staff, 1943; Sullivan et al., 2016; Watson, 1980) with an overview of fundamental magnetics theory. The mechanism of loss in magnetic devices are explained and thorough explanation of winding eddy currents, the proximity effect, a major loss mechanism in high-current, high-frequency windings is given (Bartoli et al., 1996; Dowell, 1966; Emori et al., 2013; Perry, 1979; Vandelac & Ziogas, 1987; Venkatraman, 1984). An improvement in well known steinmetz equation for core loss is introduced for non-sinusoidal transformer/inductor waveforms. The physical explanation of relaxation process is given with new loss model (Mühlethaler et al., 2011).

In many electric and electronic equipment, including computers and cell phones, inductors are crucial electric components. Industries have placed a considerable demand on inductors to reduce size, operate at higher frequencies, and have greater current tolerance. While creating new materials with superior qualities is crucial to fulfill these demands, inductor form advancements are also essential. One such work is reported in (Watanabe et al., 2010) which aims at reducing the size of inductors by evolutionary method that meet the requirements for inductance values under both weak and strong bias-current conditions.

Multiple derivative free optimization techniques are available in engineering optimization literature like particle swarm optimization, genetic algorithm, simulated annealing etc. The base paper of particle swarm optimization algorithm with its flowchart is often used as a tool to solve complex engineering problems including constraints (Shi, 2001). This refers to a class of metaheuristics algorithm that find its uses in optimizing mathematical functions with constraints. Although, a plentiful literature is available addressing the design of magnetic devices, modeling its loss components etc, design aspects achieving a particular objective need to fill the existing gap. Keeping all this in mind, an objective function is formulated in terms of core and copper loss and a derivative free metaheuristic algorithm (particle swarm optimization) has been applied to achieve an objective of determining the optimum total loss. The optimum variables, which results after solving the optimization problem are further used to compute the core dimensions. Visualization of different dimensions of ferrite cores are accessible with their computation formulas (Coil32, 2024) .

The following objectives have been achieved in the paper.

- To optimize the total loss (copper and core loss) by formulating an objective function in terms of core and copper loss
- To estimate EE type shaped ferrite core parameters based on the optimized core variables.

The paper is organized as follows. Section-2 describes the basic transformer design constraints and modeling of copper as well as core loss. Section-3 explains the step by step procedure of transformer design, followed by Section-4, which illustrates the design problem and its solution through proposed method. Section-5 concludes the paper.

2. BASIC TRANSFORMER DESIGN CONSTRAINTS

In the number of applications such as filter inductor design (shown in Fig.1(ii)), where the dominant design constraints are copper loss and saturation flux density, copper loss and saturation flux density are specified while core loss is not specifically addressed. But in the substantial class of applications such as high frequency transformer, the core loss is limited by operating flux density rather than saturation, therefore it is necessary to control the core loss by operating at reduced peak ac flux density (Erickson & Maksimovic, 2020).

Several constraint equations can be written and then combined into one equation for choosing a core. The fundamental limitations delineate the following: flux density, copper loss, core loss, and overall power loss relative to flux density regarding K- winding transformer design as shown in Fig. 1(i). The flux density is then selected, to optimize the overall power loss.

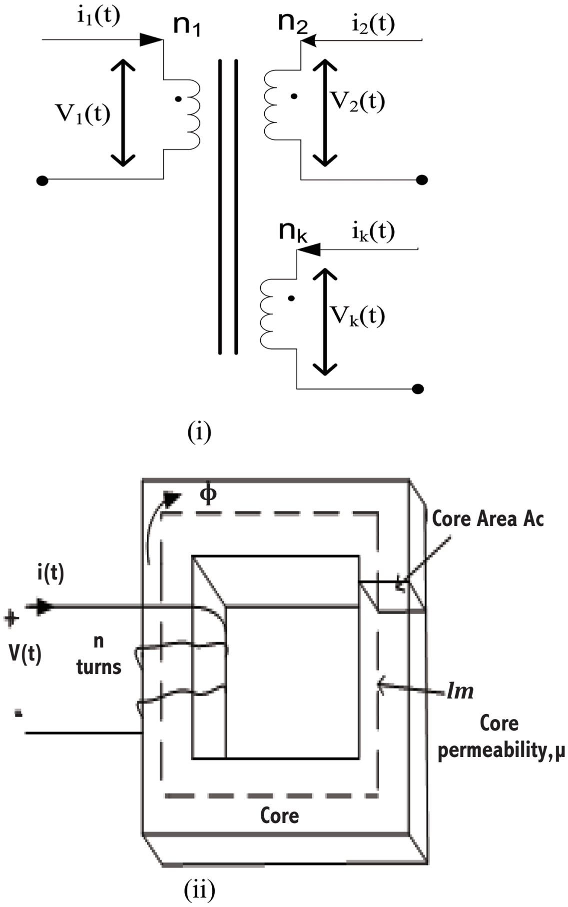

Figure 1 (i) K winding transformer with significant copper and core loss (ii) parameters of a filter inductor

2.1 Core Loss Model

Energy is required to effect a change in the magnetization of a core material. Not all of this energy is recoverable in electrical form; a fraction is lost as heat. This power loss can be observed electrically as hysteresis of the B-H loop.

Consider n-turn inductor excited by periodic waveforms v and i having frequency f. The net energy that flows into the inductor over one cycle is-

$$W = \int v . i \, dt \tag{1}$$

The equation described in (1) can be related to B-H loop characteristics. By Faraday's and Ampere's law, the following relations are written in (2).

$$v = nA_c \frac{dB}{dt} \text{ and, } i = \frac{Hl_m}{n} \tag{2}$$

substituting (2) into (1) results in (3)

$$W = A_c l_m \int H\, dB \quad (3)$$

Where, $A_c l_m$ is volume of the core and integral is area of the B-H curve. The energy lost per cycle = (volume of the core) (area of the B-H loop). Therefore, the hysteresis loss is obtained by multiplying the excitation frequency to (3), as shown in (4).

$$P_{hys} = f A_c l_m \int H\, dB \quad (4)$$

Iron alloys, that unfortunately, also function well as electrical conductors make up magnetic core materials. Electrical eddy currents may therefore flow within the core material itself as a result of ac magnetic fields. According to Lenz's law, this causes eddy currents *i(t)* to flow in directions that are opposite to the time-varying flux Φ. These eddy currents cause heat dissipation due to resistance of the core material. High-frequency applications are particularly affected by eddy current losses.

According to faraday's law, the current drives around the zigzag paths by the ac flux Φ inducing voltage in the core. The voltage magnitude rises immediately with the excitation frequency f since the induced voltage is proportional to the derivative of the flux. The induced eddy currents magnitude also rises directly with f if the core material's resistance is completely resistive and frequency-independent. This suggests that there should be an increase in eddy current losses. The core material impedance magnitude actually lowers with increasing f in power ferrite materials. The eddy current losses usually grow more quickly than f^2 over the useful frequency range.

The empirical formula of the core loss is described in (5).

$$P_{core} = K_{fe} A_c l_m \Delta B^{\beta} \quad (5)$$

Where $K_{fe} = kf^{alpha}$, alpha is property of core material and k is constant. The parameters $\boldsymbol{K_{fe}}$ and β are determined by fitting (5) to the manufacturer's published data. Where $\boldsymbol{K_{fe}}$ is the constant of proportionality whose value depend upon the operating frequency (rises with an operating frequency); $\boldsymbol{A_C}$ is cross section area of core; $\boldsymbol{l_m}$ is the mean length of magnetic path; exponent β ranges between 2 and 3 and depends on the core material. For ferrite materials functioning within their intended range of ΔB and frequency, typical values of β fall between 2.6 and 2.8. The proportional constant $\boldsymbol{K_{fe}}$ quickly rises with the frequency of excitation.

For (5), it is assumed that applied waveform signal is sinusoidal and there are no harmonic contents in the waveform (Bhambri et al., 2022; Erickson & Maksimovic, 2020; Watson, 1980). In vast applications of power electronics, voltages across transformer windings or inductors are rectangular (non-sinusoidal) in shape. This can be negative, positive or zero in some duration, resulting in ramping up, ramping down or constant flux in the core. The main limitation of (5) is that it only applies for sinusoidal excitation. In order to address core loss for non-sinusoidal waveforms, approaches are developed. One such approach is iGSE (improved generalized Steinmetz equation). According to this, improved version of (5) is shown as follows (Mühlethaler et al., 2011).

$$P_{core} = \frac{1}{T}\int_0^T K_i \left|\frac{dB}{dt}\right|^{alpha} \Delta B^{(\beta - alpha)} dt \quad (6)$$

$$K_i = \frac{k}{2\pi^{(alpha-1)} \int_0^{2\pi} |cos\theta|^{(alpha)} 2^{(\beta-alpha)} d\theta} \quad (7)$$

k, alpha, β : parameters of Steinmetz equation

2.2 Flux Density

Fig.2 shows an arbitrary periodic primary voltage waveform $v_1(t)$. The applied volt-seconds during the waveform's positive phase are indicated by the dashed area in Fig.2.

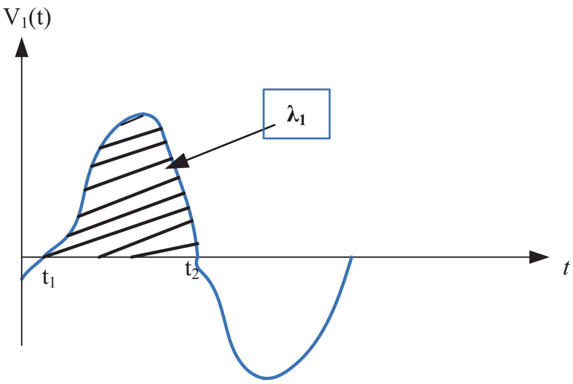

Figure 2 Volt-second applied during positive cycle of a waveform

$$\lambda_1 = \int_{t1}^{t2} v_1(t)\, dt \quad (8)$$

As a result of these volt-seconds, also known as flux-linkages, the flux density shifts from its negative maximum value to its positive maximum. The peak value of an ac component of ΔB is therefore determined by Faraday's law, described in (9).

$$\Delta B = \frac{\lambda_1}{2n_1 A_c} \tag{9}$$

Now observing, that by adding the number of turns n_1, we may minimize ΔB for a given applied voltage waveform and λ_1. This has the consequence of lowering the core loss as per (5). But, because there will be more turns of smaller wire in the new windings, it also results in an increase in copper loss. Consequently, there exists an optimum option for ΔB wherein the overall loss is reduced. We will ascertain the optimum ΔB in the sub section 2.5. After that, we can use (9) to get the primary turns n_1 as described in (10).

$$n_1 = \frac{\lambda_1}{2\Delta B\, A_c} \tag{10}$$

2.3 Copper Loss Model

The available window space must be divided among several windings in the multiple-winding scenario (shown in Fig.3) since each winding contributes a certain amount of copper loss.

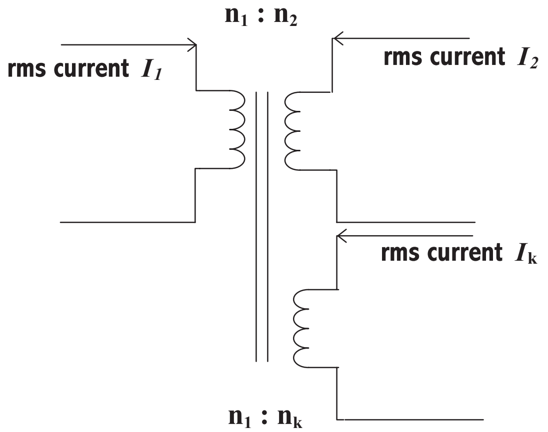

Figure 3 Magnetic element with K winding

The distribution of the window area W_A among the several windings in a multiple-winding magnetic device is the first problem to be resolved. The goal is to create a device with K windings that have turn ratios of n_1: n_2:...: n_k. The rms currents I_1, I_2, …. I_K must be conducted via these windings, respectively. It should be mentioned that the windings are essentially in parallel since the turns ratios ideally match the winding voltages. However, the loads determine the winding rms currents, which are typically not related to the turn ratios. Fig. 3 depicts the device schematically. Fig.4(i) summarizes the pertinent geometrical parameters. A portion of the total window area W_A must be assigned to each winding, as shown in Fig. 4 (ii).

Let α_j be the per unit value of the window's area allocated to winding j, where

$$\frac{v_1(t)}{n_1} = \frac{v_2(t)}{n_2} \ldots\ldots = \frac{v_k(t)}{n_k} \tag{11}$$

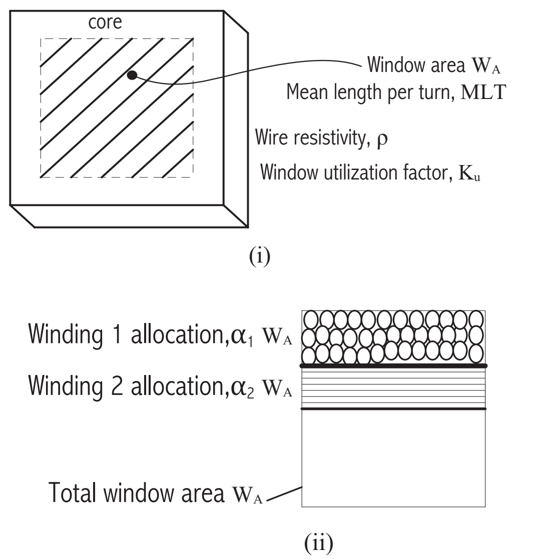

Figure 4 (i) core topology, with window area W_A (ii) allocation of window by windings to minimize low frequency copper loss

$$1 > \alpha_j > 0$$

$$\alpha_1 + \alpha_2 + \alpha_3 \ldots\ldots \alpha_k = 1 \tag{12}$$

The low-frequency loss P_{cuj} in winding j depends on the dc resistor R_j as given below-

$$P_{cuj} = I_j^2 R_j \tag{13}$$

The j[th] winding resistance is given by-

$$R_j = \frac{\rho l_j}{A_{wj}} \tag{14}$$

Where ρ is the resistivity, l_j is the j[th] winding conductor length and A_{wj} is the cross-sectional area of the j^{th} winding. The quantities are expressed below-

$$l_j = n_j\,(MLT) \tag{15}$$

$$A_{wj} = \frac{W_A K_u \alpha_j}{n_j} \tag{16}$$

Where MLT and K_u are referred to mean length per turn of the winding and window utilization factor (fill factor) respectively.

$$R_j = \frac{\rho n_j^2 (MLT)}{W_A K_u \alpha_j} \tag{17}$$

Therefore, copper loss of winding j is-

$$P_{cu,j} = i_j^2 \frac{\rho n_j^2 (MLT)}{W_A K_u \alpha_j} \tag{18}$$

Total loss in K windings is given in (19)

$$P_{cu,tot} = P_{cu1} + P_{cu2} + P_{cu3} \ldots\ldots\ldots P_{cuk}$$

$$= \frac{\rho MLT}{W_A K_u} \sum_{j=1}^{k} \left(\frac{i_j^2 n_j^2}{\alpha_j}\right) \tag{19}$$

The optimum value of α_j $(j = 1, 2 \ldots K)$ to minimize the total loss, described in (19), is stated as follows (Bhambri et al., 2022).

$$\alpha_m = \frac{n_m I_m}{\sum_{j=1}^{K} I_j n_j} \tag{20}$$

The optimum value of α, in (20) can also be expressed in terms of winding voltages as these are proportional to turns ratios.

$$\alpha_m = \frac{V_m I_m}{\sum_{j=1}^{k} I_j V_j} \tag{21}$$

Substituting the optimum value of α in (19) results in expression of total loss.

$$P_{cu} = \frac{\rho (MLT) n_1^2 I_{tot}^2}{W_A K_u} \tag{22}$$

$$\text{where, } I_{tot} = \sum_{j=1}^{K} \frac{n_j I_j}{n_1}$$

Allocating the window area of core (W_A) to the different windings based on their relative apparent powers enable to minimize the overall copper loss. (Bhambri et al., 2022; Erickson & Maksimovic, 2020; Bartoli et al., 1996).

Now, substituting n_1 (from (10)) into (22) results in (23).

$$P_{cu} = \left(\frac{\rho \lambda_1^2 I_{tot}^2}{4K_u}\right)\left(\frac{MLT}{W_A A_c^2}\right)\left(\frac{1}{\Delta B}\right)^2 \tag{23}$$

The right side of (23) is divided into three terms. First term represents the specifications; second term is a function of core geometry and last term is a function of ΔB which must be chosen to minimize P_{cu}. More ΔB results in less P_{cu} and vice versa.

2.4 Total power loss versus ΔB

The total power loss is described in (24). The dependence of ΔB on P_{fe} and P_{cu} is shown in Fig.5. It is observed from the characteristics that there is a certain flux density ΔB_{opt} at which total loss is minimum and there is a need to find such operating flux density. In the next subsection, the procedure of obtaining optimum flux density (ΔB_{opt}) is described in detail.

$$P_{tot} = P_{fe} + P_{cu} \tag{24}$$

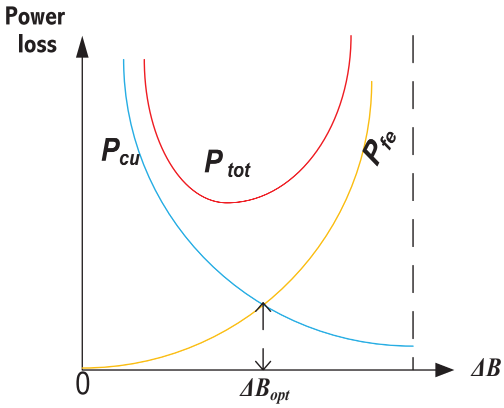

Figure 5 Total loss vs peak ac flux density

2.5 Optimum Flux Density

Differentiation of (24) is required to minimize P_{tot} for any ΔB.

Therefore, differentiating (24) results in (25).

$$\frac{dP_{tot}}{d\Delta B} = \frac{dP_{fe}}{d\Delta B} + \frac{dP_{cu}}{d\Delta B} = 0 \tag{25}$$

Here it is not a necessary condition of $P_{fe} = P_{cu}$ for optimum loss to occur, rather optimum loss occurs when

$$\frac{dP_{fe}}{d\Delta B} = - \frac{dP_{cu}}{d\Delta B} \tag{26}$$

The derivative of copper and core losses with respect to ΔB is given by (27) and (28) respectively.

$$\frac{dP_{fe}}{d\Delta B} = \beta K_{fe}(\Delta B^{\beta-1}) A_c l_m \tag{27}$$

$$\frac{dP_{cu}}{d\Delta B} = -2\left(\frac{\rho\lambda_1^2 I_{tot}^2}{4K_u}\right)\left(\frac{MLT}{W_A A_c^2}\right)\left(\frac{1}{\Delta B}\right)^{-3} \tag{28}$$

Where ρ is specific resistance in Ω-cm and MLT is the mean length per turn.

Therefore, equating (27) and (28) according to (26) results in (29).

$$\Delta B_{opt} = \left(\left(\frac{\rho\lambda_1^2 I_{tot}^2}{2K_u}\right)\left(\frac{MLT}{W_A A_c^3 l_m}\right)\frac{1}{\beta K_{fe}}\right)^{\frac{1}{\beta+2}} \tag{29}$$

the total loss is calculated by substituting ΔB, obtained in (29), in (5) and (23) respectively. Now the total loss is expressed in (30)

$$P_{tot} = (A_c l_m K_{fe})^{\frac{2}{\beta+2}}\left(\left(\frac{\rho\lambda_1^2 I_{tot}^2}{4K_u}\right)\left(\frac{MLT}{W_A A_c^2}\right)\right)^{\frac{\beta}{\beta+2}}\left(\left(\frac{\beta}{2}\right)^{\frac{-\beta}{\beta+2}} + \left(\frac{\beta}{2}\right)^{\frac{2}{\beta+2}}\right) \tag{30}$$

The above equation can be regrouped as follows in (31).

$$\frac{A_c^{2\left(\frac{\beta-1}{\beta}\right)} W_A}{(MLT)\, l_m^{\frac{2}{\beta}}}\left(\left(\frac{\beta}{2}\right)^{\frac{-\beta}{\beta+2}} + \left(\frac{\beta}{2}\right)^{\frac{2}{\beta+2}}\right)^{\frac{-(\beta+2)}{\beta}} = \frac{\rho\lambda_1^2 I_{tot}^2 \left(K_{fe}^{\frac{2}{\beta}}\right)}{4K_u\left(P_{tot}^{\frac{\beta+2}{\beta}}\right)} \quad \ldots(31)$$

The left side of (31) is regarded as core geometrical constant which depends on the geometry of the core while the right side terms contains specifications (ρ, I_{tot}, λ_1, K_u, P_{tot}) and desired core material (K_{fe}, β). The core geometrical constant is expressed in (32).

$$K_{gfe} = \frac{A_c^{2\left(\frac{\beta-1}{\beta}\right)} W_A}{(MLT)\, l_m^{\frac{2}{\beta}}}\left(\left(\frac{\beta}{2}\right)^{\frac{-\beta}{\beta+2}} + \left(\frac{\beta}{2}\right)^{\frac{2}{\beta+2}}\right)^{\frac{-(\beta+2)}{\beta}} \tag{32}$$

In order to design a transformer, K_{gfe} is estimated. A core is chosen whose K_{gfe} satisfies the following inequality, stated in (33).

$$K_{gfe} \geq \frac{\rho\lambda_1^2 I_{tot}^2 \left(K_{fe}^{\frac{2}{\beta}}\right)}{4K_u\left(P_{tot}^{\frac{\beta+2}{\beta}}\right)} \tag{33}$$

K_{gfe} is a measure of magnetic size of the core for applications where core loss is significant. It depends upon β, which varies with choice of material. For most of the high frequency ferrite cores, value of β is 2.7. Once the core type is chosen, the corresponding values of A_c, MLT, W_A, l_m are known. Now the peak value of ac flux density can be computed using (29) and number of primary winding turns (n_1) can be calculated by (10). The secondary winding turns can be calculated by using the desired turns ratio. Window space allocations and the wire gauges for the K windings can then be calculated as described in (34) and (35).

$$\alpha_m = \frac{n_m I_m}{\sum_{j=1}^{k} n_j I_j} \tag{34}$$

$$A_{wj} = \frac{K_u W_A \alpha_j}{n_j} \tag{35}$$

Where A_{wj} stands for the wire area of j^{th} winding.

3. A STEP BY STEP PROCEDURE FOR TRANSFORMER DESIGN

In this straightforward transformer design process, viewed as a first-pass method, just like the filter inductor design process, detailed insulation requirements, conductor eddy current losses, temperature rise, roundoff of number of turns, and other factors have been neglected (Bhambri et al., 2022; Erickson & Maksimovic, 2020).

Table 1 EE Core data

Core Type	Geometrical Constant (K_g) cm^5	Geometrical Constant (K_{gfe}) cm^x	Cross sectional area (A_c) cm^2	Bobbin Winding area (W_A) cm^2	Mean length per turn (MLT) cm	Magnetic path length (cm)	Weight of core (g)
EE30	$85.7.\ 10^{-3}$	$6.7.10^{-3}$	1.09	0.476	6.60	5.77	32.4
EE40	0.209	$11.8\cdot10^{-3}$	1.27	1.10	8.50	7.70	50.3
EE50	0.909	$28.4\cdot10^{-3}$	2.26	1.78	10.0	9.58	116
EE60	1.38	$36.4\cdot10^{-3}$	2.47	2.89	12.8	11.0	135

Note: Erickson & Maksimovic, 2020

A. Determination of core size

A core is selected such that it satisfies the inequality described in (36).

$$K_{gfe} \geq \frac{\rho \lambda_1^2 I_{tot}^2 (K_{fe}^{\frac{2}{\beta}})}{4K_u (P_{tot}^{\frac{\beta+2}{\beta}})} 10^8 \tag{36}$$

B. Determination of Peak flux density

$$\Delta B = (10^8 \left(\frac{\rho \lambda_1^2 I_{tot}^2}{2K_u}\right)\left(\frac{MLT}{W_A A_c^3 l_m}\right)\frac{1}{\beta K_{fe}})^{\frac{1}{\beta+2}} \tag{37}$$

ΔB can be computed by (37) ensuring that it should be less than the core's saturation flux density.

C. Evaluation of primary turns and remaining winding turns

Primary number of turns are evaluated by (38).

$$n_1 = \frac{\lambda_1}{2\Delta B\, A_c} 10^4 \tag{38}$$

Turns of remaining windings can be computed as expressed in (39).

$$n_2 = n_1 \frac{n_2}{n_1},\ n_3 = n_1 \frac{n_3}{n_1},\ \ldots\ldots \tag{39}$$

D. Window space fraction for each winding

Window space fraction, α refers to percentage of window space that each winding occupies. For a K winding transformer, these are calculated as in (40).

$$\alpha_1 = \frac{n_1 I_1}{n_1 I_{tot}},\ \alpha_2 = \frac{n_2 I_2}{n_1 I_{tot}},\ \alpha_K = \frac{n_K I_K}{n_1 I_{tot}} \tag{40}$$

E. Evaluation of wire gauge

Wire gauges are calculated according to (41).

$$A_{w1} < \frac{K_u W_A \alpha_1}{n_1},\ A_{w2} < \frac{K_u W_A \alpha_2}{n_2}, \tag{41}$$

In (41), K_u refers to the window utilization factor. The flowchart of design is shown in Fig.7.

This allows for the determination of a winding geometry and the evaluation of copper losses resulting from the proximity effect. At last, the magnetizing inductance, magnetizing current and resistance of multiple windings can be evaluated.

If these losses are substantial, it might be desirable to further optimize the design by repeating the previous steps and increasing the effective wire resistivity to the value $\rho_{eff} = \rho_{cu}(P_{cu}/P_{dc})$, where P_{dc} is the copper loss obtained when the proximity effect is minimal and P_{cu} is the actual copper loss including proximity effects.

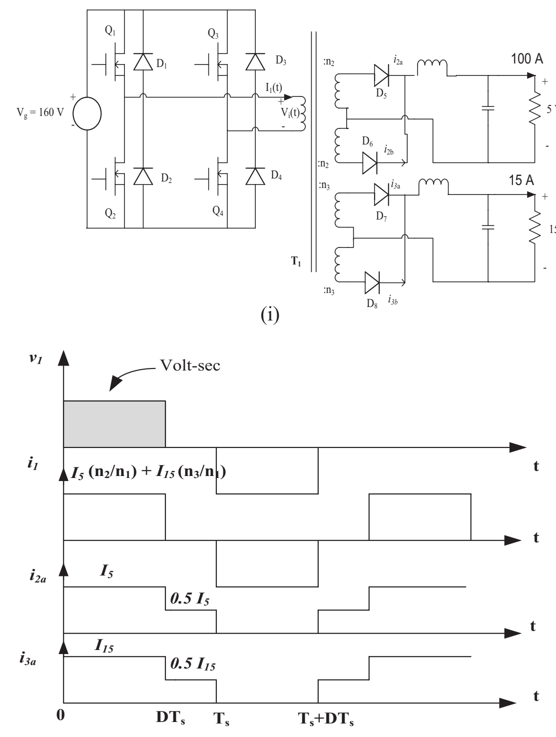

(ii)

Figure 6 (i) Circuit of multi-winding full bridge buck converter (ii) associated waveforms

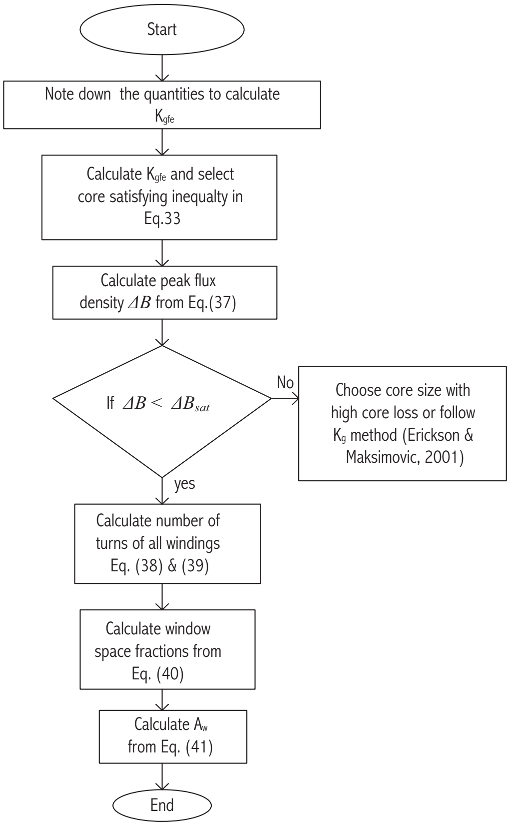

Figure 7 Flow chart of design in section-3

4. RESULT AND DISCUSSION

Transformer shown in multiple output full bridge buck converter is considered for design process. It contains five windings, one primary (n_1 turns) and two pairs (n_2 and n_3) of secondary each. The schematic is shown in Fig.6 and necessary parameters for design are given in Table.1 and Table .3 respectively. The total loss (copper + core) allowed is 4 Watt.

Quantities specified are-

n_1: n_2: n_3 (Transformer turns ratio)

K_{fe} (core loss coefficient) W/cm³T$^{\beta}$

β (exponent)

K_u (window utilization factor)

ρ (resistivity of wire used) Ω-cm

D (duty ratio)

T_s (switching time) sec

V_g (converter supply) Volt

The flux linkages are computed in (42)

$$\lambda_1 = DT_sV_g$$
$$= (0.75)(6.67\mu s)(160V) = 800\ V\mu sec \quad (42)$$

The primary RMS current is calculated as per (43).

$$I_1 = (\frac{n_2}{n_1} I_5 + \frac{n_3}{n_1} I_{15}) = 5.7A \quad (43)$$

The 5 V 2nd winding RMS current I_2 is calculated in (44)

$$I_2 = 0.5 I_5 \sqrt{1+D} = 66.1A \quad (44)$$

The 15 V 2nd winding RMS current I_3 is calculated in (45)

$$I_3 = 0.5 I_{15} \sqrt{1+D} = 9.9A \quad (45)$$

According to (6), the total RMS winding current referred to primary is calculated in (46)

$$I_{tot} = \sum_{all\ 5\ windings} \frac{n_j I_j}{n_1} = I_1 + 2\frac{n_2 I_2}{n_1} + 2\frac{n_3 I_3}{n_1} = 14.4 \text{ Amps} \quad (46)$$

The core size is evaluated as in (47)

$$K_{gfe} \geq \frac{\rho \lambda_1^2 I_{tot}^2 (K_{fe}^{\frac{2}{\beta}})}{4K_u (P_{tot}^{\frac{\beta+2}{\beta}})} 10^8 = 0.00937 \quad (47)$$

The EE type core data of Table.1 lists the EE40 core specifications with K_{gfe} = 0.0118 at β = 2.6 and satisfying the inequality described in (31). Then ΔB, Peak ac flux density is determined by (48).

$$\Delta B = \left(\left(\frac{\rho \lambda_1^2 I_{tot}^2}{2K_u} \right) \left(\frac{MLT}{W_A A_c^3 l_m} \right) \frac{1}{\beta K_{fe}} \right)^{\frac{1}{\beta+2}} = 0.23T \quad (48)$$

Peak flux density is less than saturation flux density of 0.35T. The secondary and primary number of turns are calculated as-

$$n_1 = 10^4 \cdot (800\times10^{-6})/(2\times0.23\times1.27) = 13.7 \text{ turns}$$

Hence $n_2 = \frac{5}{110} n_1 = 0.62$ and $n_3 = \frac{15}{110} n_1 = 1.87$

Table 2 AWG# data

AWG#	Area (10^{-3}) cm2	Diameter, cm	Resistance, (10^{-6}) Ω/cm
8	83.67	0.326	20.6
15	16.51	0.153	104.3
16	13.07	0.137	131.8
17	10.39	0.122	165.8
18	8.228	0.109	209.5
19	6.531	0.0948	263.9

Note: Erickson & Maksimovic, 2020

Table 3 Design parameters

Parameters	Values	Meaning
Converter output voltages	5, 15 V	
D	0.75	Duty ratio
Switching frequency	150	KHz
Turns ratio (n_1:n_2:n_3)	110:5:15	
K_{gfe}	7.6	Core geometrical constant, W/T^{β} cm^3
K_u	0.25	Window utilization factor
P_{tot}	4	Watt
β	2.6	exponent
ρ (rho)	1.724	

Note: Erickson & Maksimovic, 2020

Since transformer has turns ratio of 110:5:15. In practicality, we should select n_1 = 22,

n_2 = 1 and n_3 = 3.

Now ΔB = 10^4.(800×10^{-6})/(2×22×1.27) = 0.143 Tesla. The resulting copper loss and core loss can be computed using (22) and (5) which results in P_{fe} = 0.47 W, P_{cu} = 5.4 W and P_{tot} = 5.9 W. This is fifty percent more than the design objective of 4W, it is essential to increase the core size. The next bigger EE core is EE50 core, having K_{gfe} of 0.0284. With n_1 = 22, it leads to peak flux density of ΔB = 0.08 T. The resulting power losses are P_{fe} = 0.23 W and P_{cu} = 3.89 W so that P_{tot} = 4.12 W.

With the core EE50 and n_1 = 22, the window space fractions of transformer windings are computed by (49).

$$\alpha_1 = \frac{I_1}{I_{tot}} = 0.396,\ \alpha_2 = \frac{n_2}{n_1}\frac{I_2}{I_{tot}} = 0.209,$$

$$\alpha_3 = \frac{n_3}{n_1}\frac{I_3}{I_{tot}} = 0.094 \tag{49}$$

The primary 110V wire gauge area (A_{w1}), secondary 5 V wire area (A_{w2}) and secondary 15 V wire area (A_{w3}) can be then calculated according to (41).

$$A_{w1} = \frac{(0.25).(1.78).(0.39)}{22} = (8).(10^{-3})\ \mathrm{cm}^2$$

$$A_{w2} = \frac{(0.25).(1.78).(0.39)}{1} = (93)\ (10^{-3})\ \mathrm{cm}^2$$

$$A_{w1} = \frac{(0.25).(1.78).(0.094)}{3} = (13.9)\ (10^{-3})\ \mathrm{cm}^2$$

The type of wires used for different windings are selected according to AWG (American wire gauge) data given in Table.2 AWG #19 can be selected for primary winding followed by AWG #8 and AWG # 16 for the rest two secondary windings respectively. Although it would likely be simpler to utilize a flat copper foil winding, the 5V windings might be wound using numerous rounds of smaller paralleled wires. Interleaving multiple thin layers of foil with the primary winding can reduce proximity losses if insulation needs permit.

4.1 Optimizing Total loss using Core parameters as variables

To further reduce the total loss, the design procedure discussed above has been turned into an optimization problem with constraints. A metaheuristics algorithm is applied to solve this minimization problem to find a set of core variables.

fnc-function,

The transformer copper and core loss functions are described in (50) and (51) respectively.

$$P_{cu} = fnc(I_{tot}, \mathrm{MLT}, W_A, A_c, \Delta B) \tag{50}$$

$$P_{fe} = fnc\ (\Delta B, A_c, l_m) \tag{51}$$

Where *MLT* is mean length per turn in cm; W_A is window area in cm^2; A_c is core cross-sectional area in cm^2 and l_m is mean length in cm respectively. The peak flux density function is described in (52).

$$\Delta B = fnc\ (\alpha_1, \alpha_2, \alpha_3, \text{MLT}, W_A, A_c, l_m) \tag{52}$$

Now, the objective is to minimize the total loss (core and copper loss), stated in (53).

$$\text{Objective Function- } \min\ (P_{cu} + P_{fe}) \tag{53}$$

subject to inequality and equality constraints, which are described in (54) (Bhambri et al., 2022)

$$K_{gfe} \geq \frac{\rho \lambda_1^2 I_{tot}^2 (K_{fe}^{\frac{2}{\beta}})}{4K_u (P_{tot}^{\frac{\beta+2}{\beta}})}\ ,\ \Delta B \leq \Delta B_{sat}$$

$$\text{and } \alpha_1 + 2\alpha_2 + 2\alpha_3 = 1,$$

$$I_{tot} = \sum_{all\ K\ windings} \frac{I_j n_j}{n_1} \tag{54}$$

Where, $I_{tot}\ \alpha\ (\alpha_1\ , \alpha_2,\ \alpha_3)$

4.2 Proposed metaheuristics algorithm

A succinct overview of PSO algorithm is given below.

4.2.1 PSO: Particle swarm optimization is population based derivative free metaheuristics algorithm that is inspired by bird flocking or fish schooling behavior. At start of the algorithm, population (parameters) and their velocities are initialized randomly in feasible range and their fitness values are calculated. Velocity is calculated and population is updated at each iteration as per (55) and (56). Best fit particles are replaced by worst fit and then algorithm goes to the next iteration (Shi, 2001) The various parameters used in the PSO algorithm are shown in Table.4.

Table 4 PSO parameters

Parameter	Meaning	Value
C_1 and C_2	Acceleration coefficients	2
ω	Inertia factor	W_{max}: 0.9 W_{min}: 0.4
iter	iterations	1200
pop	population	30

$$vel_{i,j}^{iter} = \omega^{iter}.\ vel_{i,j}^{iter} + c_1\ (pbest_{i,j}^{iter} - pop_{i,j}^{iter}) + c_2 (gbest_{i,j}^{iter} - pop_{i,j}^{iter}) \tag{55}$$

$$pop_{i,j}^{iter} = pop_{i,j}^{iter} + vel_{i,j}^{iter} \tag{56}$$

Where *vel, pbest* , *pop* and *gbest* are velocity, personal best , population and global best i^{th} particle. *i* ,*j* and *iter* are particle, dimension and iteration number respectively. ω^{iter} is linearly decreasing inertia factor (Shi, 2001). The optimized core variables and corresponding total loss are shown in Table.5. The variation of the fitness function with algorithm iterations is shown in Fig.8. The flowchart of the design is shown in Fig.10. The wire gauges for different windings can be selected as discussed in the section-4.

Table 5 Optimized core variables and total loss

Initializing range of core variables	Optimized core variables	P_{cu}, P_{fe} and Total Loss	P_{tot} without PSO	Optimized ΔB
A_c: (1.5 - 3)cm^2	1.8872	P_{cu} = 1.8498 P_{fe} = 0.3919 Total loss = 2.2417 W	4.12 W	0.0963
W_A: (1 - 3)cm^2	3			
MLT: (8 - 10)cm	8			
lm: (10 - 12)cm	11.9861			
α_1, α_2, α_3: (0 - 1)	0.3956, 0.2085, 0.0937			

After comparing the total loss incurred, it is clear that designed core variables results in significant reduced (45.6% less) loss (see Table.5).

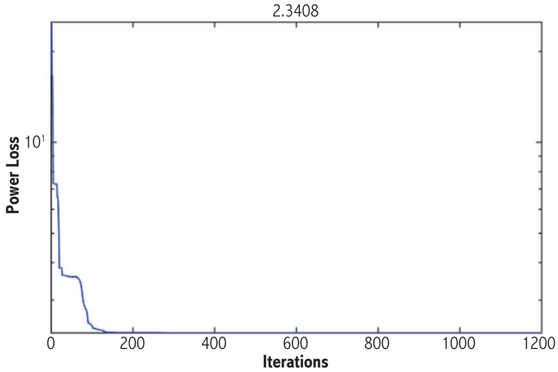

Figure 8 Fitness function vs iterations

The variation in optimized optimized flux density (ΔB) for distinct mean length (l_m) of magnetic path and core cross-sectional area (A_c) is shown in Fig.11. It is observed that optimized flux density (ΔB) goes on decreasing as the size (volume) of core increases. However, the optimized power loss (P_{tot}) remains nearly same. The geometrical constants, satisfying the inequality, stated in (33) and total loss for various designs are shown in Table.6. It is inferred by observing Eq. 29 that optimum flux density (ΔB_{opt}) is a function of switching frequency. The significant increase in switching frequency (f_{sw}) will reduce applied volt-sec (λ_1) and increase K_{fe} simultaneously. As a result of this, the optimum B reduces according to (29).

The magnetizing inductance ($\mathrm{L_M}$) and magnetizing current, shown in Fig.9 can be calculated by expressions stated in (57) and (58).

$$\mathrm{L_M} = \mu \frac{\mathrm{n}_1^2 A_c}{l_m} \tag{57}$$

$$i_{Mpeak} = \frac{\lambda}{2\mathrm{L_M}} \tag{58}$$

The variation in the magnetizing inductance and current for various designs, shown in Table.6, with optimum flux density is shown in Fig.12. It is observed that as the size (volume) of core increases, magnetizing inductance decreases and current increases.

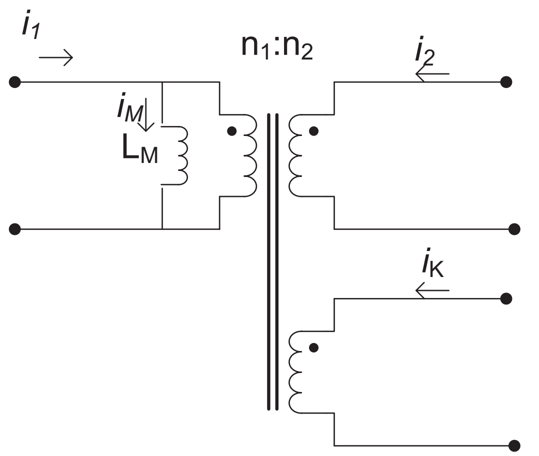

Figure 9 magnetizing inductance $\mathrm{L_M}$

4.2.2 Saturation Mechanism in Transformer:

When the core flux density ΔB surpasses the saturation flux density B_{sat}, the transformer saturates and transformer windings become short circuits, the magnetizing current i_M increases, and the impedance of the magnetizing inductance decreases. It should be observed that saturation is not always caused by significant winding currents (i_1 and i_2); if these currents follow MMF equation of an ideal transformer, $\mathrm{MMF} = \Phi .\ \mathrm{R_c}$, the magnetizing current is zero and the core is not net magnetized. Instead, a transformer's saturation depends on the applied volt-seconds.

$$i_{\mathrm{M}} = \frac{1}{\mathrm{L_M}} \int \mathrm{v}_1\,(\mathrm{t}), \tag{59}$$

substituting the value of $\mathrm{L_M}$ from (57) into (59), results in (60).

or $$B = \frac{1}{A_c \mathrm{n}_1} \int \mathrm{v}_1\,(\mathrm{t}), \tag{60}$$

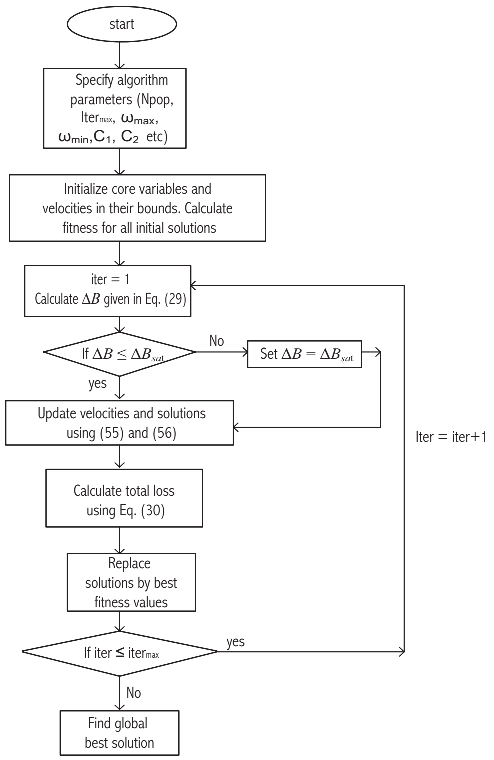

Figure 10 Flowchart of proposed design

A saturating transformer should be fixed by either raising the core cross-sectional area $\mathrm{A_c}$ or increasing the number of turns in order to reduce the flux density. Since adding an air gap does not alter Eq. (60), it has no influence on the saturation of conventional transformers. Transformer saturation is determined by the applied winding voltage waveforms rather than the applied winding currents, which sets it apart from inductor saturation mechanism.

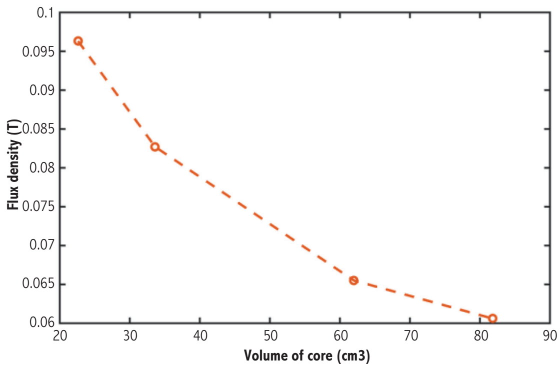

Figure 11 volume of core vs optimum flux density

Table 6 optimized core variables with distinct l_m, A_c

core variables	Optimized core variables			
	Design-1	Design-2	Design-3	Design-4
A_c (cm^2)	1.8872	2.1975	2.7776	3
W_A (cm^2)	3	2.9999	3	3
MLT (cm)	8	8.0027	8	8
l_m (cm)	11.9861	15.2947	22.3220	27.2761
α_1, α_2, α_3: (0 - 1)	0.3956, 0.2085, 0.0937	0.3956, 0.2085, 0.0937	0.3956, 0.2085, 0.0937	0.3956, 0.2085, 0.0937
ΔB	0.0963	0.0827	0.0655	0.0606
K_{gfe} (Eq.32)	0.0361	0.0361	0.0360	0.0339
K_{gfe} (Eq.33)	0.0262	0.0261	0.0261	0.0255
P_{tot}	2.2417	2.2425	2.2434	2.2746

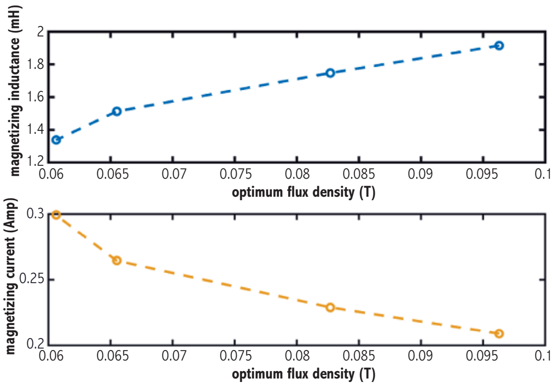

Figure 12 magnetising inductance, magnetising current vs optimum flux density

4.2.3 Determining dimensions of EE type ferrite core

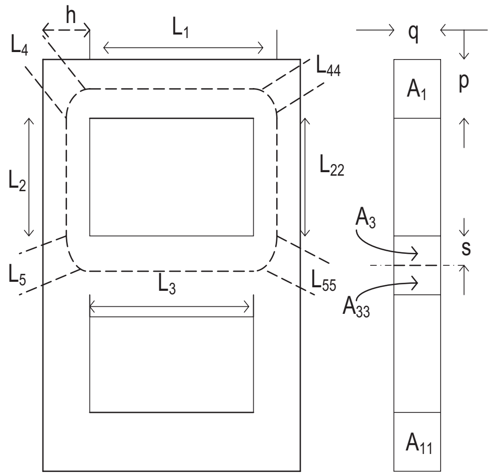

Figure 13 Dimensions of EE type ferrite core

The schematic of EE type ferrite core is shown in Fig.13. The relevant cross-section areas (cm^2) and magnetic flux path lengths (cm) of the sections can be determined using the following formulas in Eq. 61-67. The computed values are shown in Table.7 (Coil32, 2024).

$$l_1 = L_1,\ \ l_3 = L_3$$
$$l_2 = L_2 + L_{22};$$
$$l_4 = L_4 + L_{44};\ l_4 = \frac{\pi}{4}(p+h) \tag{61}$$

$$l_5 = L_5 + L_{55};$$
$$l_5 = \frac{\pi}{4}(s+h)\ \text{(for rectangular centre leg)} \tag{62}$$
$$a_1 = A_1 + A_{11};\ a_1 = 2qp,\ a_2 = 2qh$$

$$a_3 = A_3 + A_{33},\ a_3 = 2qs, \quad (63)$$
$$a_4 = (a_1+a_2)/2,\ a_5 = (a_3+a_2)/2$$

$$C_1 = \sum_{i=1}^{5} \frac{l_i}{a_i},\ C_2 = \sum_{i=1}^{5} \frac{l_i}{a_i^2} \quad (64)$$

Effective magnetic path length, $l_e = \frac{C_1^2}{C_2}$ (65)

Effective volume of core, $V_e = \frac{C_1^3}{C_2^2}$ (66)

Effective core area, $A_e = \frac{C_1}{C_2}$ (67)

Table 7 estimated core dimensions for solution shown in Table.5

Core dimensions	Values (cm)
l_1, l_3	3.3169
l_2	1.8089
q	0.5465
p	1.7268
h	0.9443
s	1.7268

5. CONCLUSION AND FUTURE WORK

This paper proposed a design methodology for an inbuilt multi-winding transformer mounted on power electronics based converter. The method is followed by selection of geometrical core constant , peak flux density, window space fractions, number of turns and then wire gauges for each winding. Entire design procedure is discussed through taking an example of multi winding full bridge buck converter. Further, this design has been turned into an optimization problem , solved for optimum core parameters like window area, core cross section area, mean length per turn, mean magnetic path and window space fractions to minimize the total loss. A metaheuristics based PSO algorithm is applied to minimize an objective function for a set of core variables with satisfying an equality and inequality constraints simultaneously. The resulting total loss is found to be much less than that of obtained through conventional method. Based on the resulting core variables, different dimensions are estimated for EE shaped ferrite core. In future work, the loss model is likely to be amended with consideration of skin and proximity effects, layer geometry, and winding technology, thermal coupling and electromagnetic interference (EMI) implications, cost analysis which are critical in practical high-frequency designs. The hardware prototype and Finite element magnetics validation are also likely to be added.

Abbreviations

K_g: Effective electrical size of core
K_{gfe}: Core geometrical constant
MLT: mean length per turn
P_{fe}: core loss
P_{cu}: copper loss
P_{tot}: total loss
ΔB: peak flux density
λ: flux linkages
n_1, n_2, n_3: number of turns in winding-1, 2 and 3
A_c: core cross sectional area
W_A: area of window
α: window space fraction
l_m: mean length of magnetic path
I_{tot}: total current
K_u: window utilization factor
ρ: resistivity
D: duty ratio
β: exponent
T_s: sampling time
V_g: voltage
PSO: particle swarm optimization
T: tesla
RMS: root mean square
HF: high frequency
EV: Electric Vehicle
cm: centimeter
MMF: magnetomotive force
R_c **:** core reluctance

Declaration: The authors declare that they have no known competing financial interests or personal relationships that could have appeared to influence the work reported in this paper. No funding has been received to carry out the written draft of the manuscript.

REFERENCES

Atalla, A., Agamy, M., Dame, M., Hao, L., Mandrisiak, G., Weeber, K., & Pan, Y. (2016, September). Advancements in high power high frequency transformer design for resonant converter circuits. In *2016 IEEE Energy Conversion Congress and Exposition (ECCE)* (pp. 1-8). IEEE. https://doi.org/10.1109/ECCE.2016.78548335.

Bartoli, M., Reatti, A., & Kazimierczuk, M. K. (1996, October). Minimum copper and core losses power inductor design. In *IAS'96. Conference Record of the 1996 IEEE Industry Applications Conference Thirty-First IAS Annual Meeting* (Vol. 3, pp. 1369-1376). IEEE. https://doi.org/10.1109/IAS.1996.559244

Bhambri, S., Shrivastava, V., & Kumawat, M. (2022, November). Design methodology of single and multi-winding coupled inductor in switching converters. In *2022 IEEE 10th Power India International Conference (PIICON)* (pp. 1-6). IEEE.

Coil32. (2024). *Ferrite E core coil calculator*. Retrieved August 1, 2024, from https://coil32.net

Dauhajre, A., & Middlebrook, R. D. (1986, June). Modelling and estimation of leakage phenomena in magnetic circuits. In *1986 17th Annual IEEE Power Electronics Specialists Conference* (pp. 213-226). IEEE.

Dhole, A., Roy, S. K., & Basu, K. (2021). Estimation and Measurement of Power Loss in a High Frequency Inductor for a DAB based DC-DC Converter. In *2021 National Power Electronics Conference (NPEC)*. (pp. 1-6). IEEE

Dowell, P. L. (1966, August). Effects of eddy currents in transformer windings. In *Proceedings of the Institution of electrical Engineers* (Vol. 113, No. 8, pp. 1387-1394). IEE. https://doi.org/10.1049/piee.1966.0236

Emori, K., Shimizu, T., & Bizen, Y. (2013, November). Discussion on design optimization of inductor loss focused on copper loss and iron loss. In *2013 1st International Future Energy Electronics Conference (IFEEC)* (pp. 241-245). IEEE. https://doi.org/10.1109/IFEEC.2013.6687510

Erickson, R. W., & Maksimovic, D. (2020). *Fundamentals of power electronics*. Springer International Publishing.

Iyer, V. M., Prabhakaran, S., & Vijayan, P. (2015, September). High-frequency, high-current transformer designs for Silicon Carbide based LLC converters. In *2015 IEEE Energy Conversion Congress and Exposition (ECCE)* (pp. 5650-5656). IEEE. https://doi.org/10.1109/ECCE.2015.7310454

Kudaravalli, V. R., Uttam, V., & Iyer, V. M. (2022, December). A design methodology for triple active bridge dc-dc converter. In *2022 IEEE International Conference on Power Electronics, Drives and Energy Systems (PEDES)* (pp. 1-7). IEEE. https://doi.org/10.1109/PEDES56012.2022.10080029

MIT Staff. (1943). *Magnetic Circuits and Transformers: A First Course for Power and Communication Engineers*. MIT Press.

Mühlethaler, J., Biela, J., Kolar, J. W., & Ecklebe, A. (2011). Improved core-loss calculation for magnetic components employed in power electronic systems. *IEEE Transactions on Power electronics*, *27*(2), 964-973. https://doi.org/10.1109/TPEL.2011.2162252.

Parikshith, B.C., Krishnan, A., John V., Karanth, A. (2010, June). An integrated design procedure for high frequency ac inductors for inverters. In *National Power Electronics Conference 2010*. IIT Roorkee.

Perry, M. P. (1979). *Multiple layer series connected winding design for minimum losses*. IEEE Transactions on Power Apparatus and systems, (1), 116-123.

Roja, P., Ansari, M. S., Venkatramanan, D., & John, V. (2024, August). Design comparison and investigations into thermal failure of HF transformers in isolated dc-dc converters. In *2024 IEEE International Communications Energy Conference (INTELEC)* (pp. 1-6). IEEE.

Shi, Y. (2001, May). Particle swarm optimization: developments, applications and resources. In *Proceedings of the 2001 congress on evolutionary computation (IEEE Cat. No. 01TH8546)* (Vol. 1, pp. 81-86). IEEE. https://doi.org/10.1109/CEC.2001.934374

Sullivan, C. R., Reese, B. A., Stein, A. L., & Kyaw, P. A. (2016, June). On size and magnetics: Why small efficient power inductors are rare. In *2016 International Symposium on 3D Power Electronics Integration and Manufacturing (3D-PEIM)* (pp. 1-23). IEEE. https://doi.org/10.1109/3DPEIM.2016.7570571

Vandelac, J. P., & Ziogas, P. (1987). A novel approach for minimizing high-frequency transformer copper losses. In *1987 IEEE Power Electronics Specialists Conference* (pp. 355–367). https://doi.org/10.1109/PESC.1987.7077203

Venkatramanan, D. & John, V. (2013), Integrated higher-order pulse-width modulation filter–transformer structure for single-phase static compensator. IET Power Electronics, 6: 67-77. https://doi.org/10.1049/iet-pel.2011.0430

Venkatraman, P. S. (1984). Winding eddy current losses in switch mode power transformers due to rectangular wave currents. In *1984 Proceedings of Powercon 11* (pp. 1-11).

Watanabe, K., Campelo, F., Iijima, Y., Kawano, K., Matsuo, T., Mifune, T., & Igarashi, H. (2010). Optimization of inductors using evolutionary algorithms and its experimental validation. *IEEE Transactions on Magnetics*, *46*(8), 3393-3396. https://doi.org/10.1109/TMAG.2010.2044986

Watson, J. K. (1980). *Applications of magnetism.* John Wiley & Sons.